

# Nanostructured Spinel $Mg_{0.7}Zn_{0.3}Fe_2O_4$ Thick Film For Ammonia Sensing

T.R. Tatte<sup>1\*</sup>, V.D.Kapse<sup>2</sup>

<sup>1</sup>Department of Physics, Shri Dr. R.G. Rathod Art and Science College, Murtizapur-444107 Maharashtra state, India.

<sup>2</sup>Department of Physics, Arts, Science and Commerce College, Chikhaldara-444807, Maharashtra State, India

*trupti.tatte@rediffmail.com*

**Abstract-** Nanocrystalline  $Mg_{0.7}Zn_{0.3}Fe_2O_4$  powder was prepared by using sol-gel method. The structure and the crystal phase of the powder were examined by X-ray diffraction (XRD). The average crystallite size was found to be 30 nm from the XRD pattern. Further investigations were carried by using Fourier Transform Infrared Spectroscopy (FT-IR). Size and shape were analyzed by a transmission electron microscopy (TEM). Thick films based on nanocrystalline mixed oxide  $Mg_{0.7}Zn_{0.3}Fe_2O_4$  were fabricated by screen printing technique and characterized by using Scanning electron microscopy (SEM) with energy dispersion X-ray analysis (EDX). Ammonia gas sensing characteristics of nanosized  $Mg_{0.7}Zn_{0.3}Fe_2O_4$  based thick films were investigated. Sensor element based on Nanosized  $Mg_{0.7}Zn_{0.3}Fe_2O_4$  was observed to be highly sensitive towards 100 ppm ammonia gas at 200°C. The quick response and fast recovery are the main features of this sensor element. The effect of microstructure and additive concentration on the gas response, selectivity, response time and recovery time of the sensor element in the presence of ammonia gas were studied and discussed.

**Keywords:**  $Mg_{0.7}Zn_{0.3}Fe_2O_4$ , TEM, Thick film, Ammonia gas sensor, Gas response.

## 1. INTRODUCTION

Gas sensors have become an integral part of the modern civilization due to their key role in detecting, monitoring, and controlling the hazardous/poisonous gases from the surrounding. Metal oxides based semiconductor gas sensors have been widely investigated for their gas sensing properties. Like other metal oxides, zinc oxide, tin oxide and tungsten oxide have been widely studied for their gas sensing applications. However, presently many other oxides have also been explored for the gas sensing devices. Recently, few reports have appeared on the ferrites as gas sensors [1–8].

Ferrite compounds are very important materials due to their semiconducting and ferromagnetic properties. Recently spinel ferrites have been found as perspective gas sensor materials at elevated temperatures [9-14]. However, the researchers are still facing cross sensitivity toward non-targeted gases, high sensitivity to humidity, long term drift towards oxygen bulk diffusion, and transformations of the crystal structure in polycrystalline materials, are the major ones [15-17]. Spinel ferrites,  $MFe_2O_4$  (M = Mg, Mn, Fe, Co, Ni, Zn, Cu, Cd, etc.) are a technologically important group of materials. Among different ferrites, magnesium ferrite ( $MgFe_2O_4$ ) enjoys a special attention because of its vast applications in high density recording media, heterogeneous catalysis, adsorption, sensors and magnetic technologies.  $MgFe_2O_4$  is a partially inverse spinel and its degree of inversion is sensitive to the thermal history of the sample, microstructure and preparative parameters.

There are several methods for synthesizing nanosized spinel ferrite particles. To prepare nanoferrites with simple routes by using cheap, non-toxic and eco-friendly precursors are still the core issue, among other proven synthesis methods [18]. Among these methods, the nanoparticles prepared by sol-gel method have been studied, although this synthesis provides a quick and easy way to prepare nanoparticle, it usually produces sample with large size distribution and less defined crystal chemistry. These nanoparticle based sensors have number of advantages such as high sensitivity, selectivity, fast response and recovery, which set them apart from the conventional gas sensors [2]. However, to our knowledge the ammonia gas-sensing characteristics of Zn doped  $\text{MgFe}_2\text{O}_4$  have been rarely reported in the open literature.

Herein, the purpose of this work is to prepare nanocrystalline Zn doped Mg spinel ferrite by a sol-gel method with a low calcination temperature involving low cost metal nitrates as raw materials and study of their structural and gas sensing properties.

## II. EXPERIMENTAL

### 2.1. Material and Methods

Nanocrystalline  $\text{Mg}_{0.7}\text{Zn}_{0.3}\text{Fe}_2\text{O}_4$  powder was prepared by the sol-gel technique. All chemicals were of analytical grade and were used without further purification. The stoichiometric molar amounts of Ferric nitrate [ $\text{Fe}(\text{NO}_3)_3 \cdot 9\text{H}_2\text{O}$ ], Magnesium nitrate [ $\text{Mg}(\text{NO}_3)_2 \cdot 6\text{H}_2\text{O}$ ], Zinc nitrate [ $\text{Zn}(\text{NO}_3)_2 \cdot 6\text{H}_2\text{O}$ ] and Citric acid [ $\text{C}_6\text{H}_8\text{O}_7 \cdot \text{H}_2\text{O}$ ] were weighed separately with a ratio 0.5M:0.25M:0.5M. All the reagents were mixed with distilled water and desired volume of mixture was prepared. Obtained mixture was stirred and heated at required temperature for 3 h and followed by heating at  $80^\circ\text{C}$ , until the mixture changed into gel formation. Then, the gel was dried in an electric oven at  $100^\circ\text{C}$  for 24 h. The obtained powder was then calcined in a muffle furnace at  $700^\circ\text{C}$  for 2 h to improve the crystallinity of the prepared material. Finally, brown colour powder was obtained. Taken solid phase sample was grinded in a mortar to make it powder for further analysis.

### 2.2. Materials Characterization

The phase confirmation was determined using X-ray diffractometer (Bruker, AXD D8-Discover using  $\text{Cu K}\alpha$  radiation with an accelerating voltage 40 kV). FT-IR image was recorded using 3000 Hyperion Microscope with Vertex 80 (Bruker, Germany) to provide information about the structural coordination in the powder sample. The TEM image was recorded using CM 200 (Philips) with an accelerating voltage of 20-200 kV.

### 2.3. Fabrication of sensor element and measurement of gas-sensing properties

Appropriate quantity of mixture of organic solvents such as butyl cellulose, butyl carbitol acetate and turpineol was added to the mixture of  $\text{Mg}_{0.7}\text{Zn}_{0.3}\text{Fe}_2\text{O}_4$  and a solution of ethyl cellulose (a temporary binder). The mixture was then ground to form paste. The obtained paste was screen printed onto a glass substrate in desired patterns. Prepared thick films were fired at  $500^\circ\text{C}$  for 1 h. Surface morphology of thick film was observed by using Scanning Electron Microscope (JSM-7600F microscope) with an accelerating voltage of 0.1 to 30 kV.

## III. RESULTS AND DISCUSSION

### 3.1. XRD analysis

Fig. 1 depicts the XRD pattern of nanocrystalline  $\text{Mg}_{0.7}\text{Zn}_{0.3}\text{Fe}_2\text{O}_4$  powder prepared by sol-gel method. XRD pattern shows the spinel structure in accordance with JCPDS card. Main characteristic peaks were found at  $2\theta$  values =  $29.90^\circ$ ,  $35.21^\circ$ ,  $56.58^\circ$ ,  $62.14^\circ$  and  $73.48^\circ$  which were identified as corresponding to Miller index (220), (311), (400), (511) and (440) respectively (JCPDS card no. 73-2211). The XRD peaks and their positions with the calculated lattice parameter confirmed that

all the compositions exhibit single-phase cubic spinel structure with  $Fd3m$  space group. No peaks from other phases are detected, indicating high purity of the products.

The average crystallite size ( $D$ ) was calculated from XRD peaks broadening using the Debye-Scherrer approximation, which is defined as  $D = K\lambda/\beta\cos\theta$ ; where  $D$  is the average crystallite size,  $k$  is a constant equal to 0.9,  $\lambda$  is the X-ray wavelength and  $\beta$  is the peak full width at half maximum (FWHM) and  $\theta$  is the angle of diffraction.

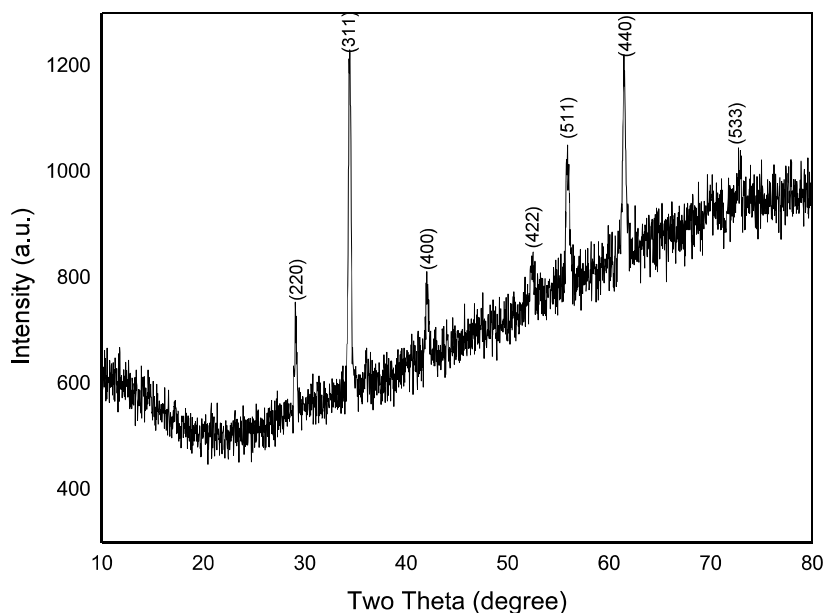


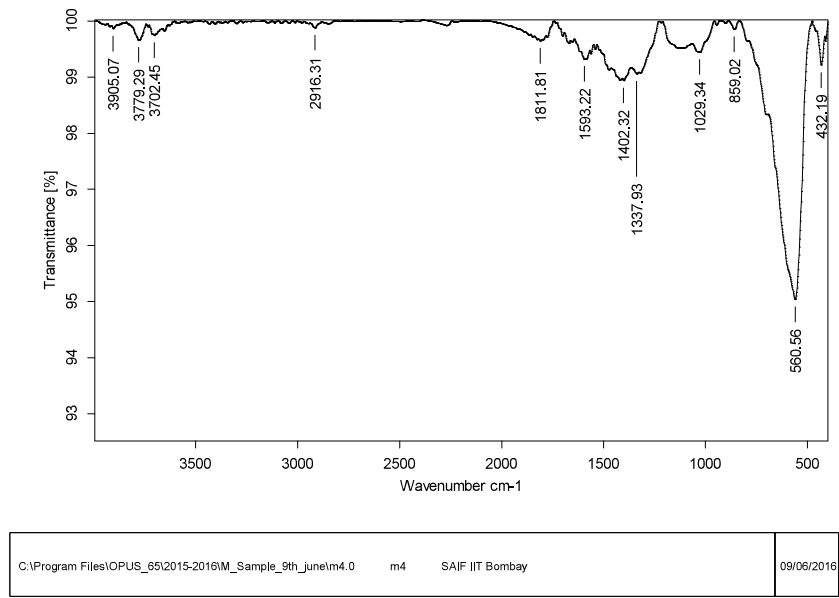
Fig. 1: XRD pattern of  $Mg_{0.7}Zn_{0.3}Fe_2O_4$  calcined at  $700^\circ C$ .

However, the lattice constant of as-synthesized ferrite powder was  $a = 8.421 \text{ \AA}$ . A similar linear variation of lattice constant with Zn content has been observed by El-Sayed [19] and Kakatkar et al. [20] for  $M-Zn$  ferrites with  $M = Ni, Co, Cu, Mg$ . The average crystallite size was determined from the XRD pattern using Debye-Scherrer formula and was found to be 30 nm.

### 3.2. FT-IR analysis

FT-IR spectra of  $Mg_{0.7}Zn_{0.3}Fe_2O_4$  nanoparticle are presented in Fig. 2. Vibrations of ions in the crystal lattice are usually observed in the range of  $4000 - 400 \text{ cm}^{-1}$  in IR analysis. Two main broad metal-oxygen bands are seen in the IR spectra relative to spinel ferrite compounds. The highest one observed in the range  $560 \text{ cm}^{-1}$ , corresponds to intrinsic stretching vibrations of the metal at the tetrahedral site, whereas the lowest band usually observed in the range  $432 \text{ cm}^{-1}$ , is assigned to octahedral-metal stretching. The  $Mg^{2+}$  ions occupy mainly the octahedral sites but fraction of these ions may be migrated into tetrahedral sites. This would explain the existence of a weak shoulder in the range of  $690 - 710 \text{ cm}^{-1}$ . This confirms that the Mg ferrite has a partially inverse spinel structure.

Content of this meant for your information and should not be used for advertisement, evidence or litigation



Page 1/1

Fig. 2: FT-IR spectra of nanosized Mg<sub>0.7</sub>Zn<sub>0.3</sub>Fe<sub>2</sub>O<sub>4</sub>.

### 3.3. SEM analysis

SEM technique was employed for finding morphology of the thick film. Fig. 3 shows SEM image of the nanocrystalline spinel Mg<sub>0.7</sub>Zn<sub>0.3</sub>Fe<sub>2</sub>O<sub>4</sub>. The SEM technique was employed for finding morphology of the powder; it shows formation of the agglomerated particle having size ~ 125 nm. SEM pictures show that the samples exhibit large grains structure having regular morphology (polygons) with the presence of soft agglomerations.

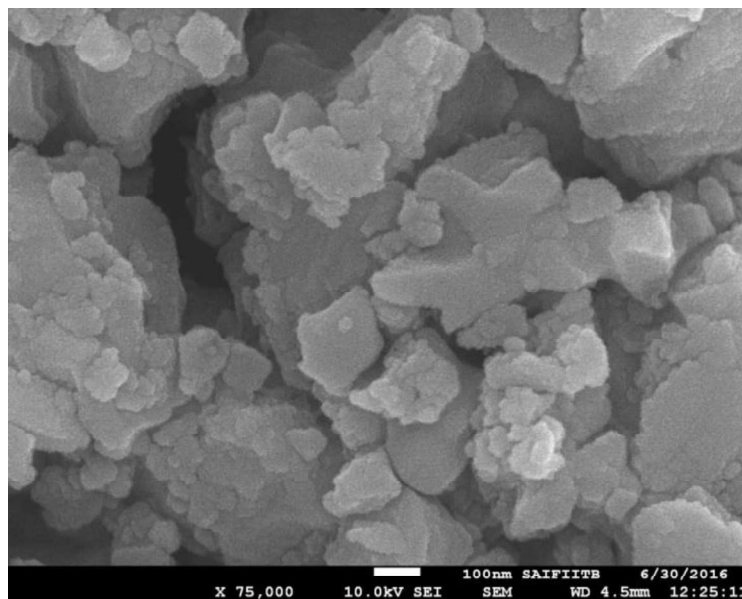


Fig. 3: SEM image of nanosized Mg<sub>0.7</sub>Zn<sub>0.3</sub>Fe<sub>2</sub>O<sub>4</sub>.

### 3.4. Energy dispersion X-ray analysis

The elemental composition of synthesized  $Mg_{0.7}Zn_{0.3}Fe_2O_4$  nanoparticle has been investigated by the energy dispersion X-ray analysis (EDX). Fig. 4 shows EDX patterns of the nanosized spinel  $Mg_{0.7}Zn_{0.3}Fe_2O_4$ . From the EDX spectrum, the presence of Mg, Zn, Fe and O has been confirmed and EDX results reveal almost the same ratio of Mg/Zn/Fe for the synthesized nanoparticle as they were actually added during synthesis process. Hence, confirms the purity of nanocrystalline  $Mg_{0.7}Zn_{0.3}Fe_2O_4$ .

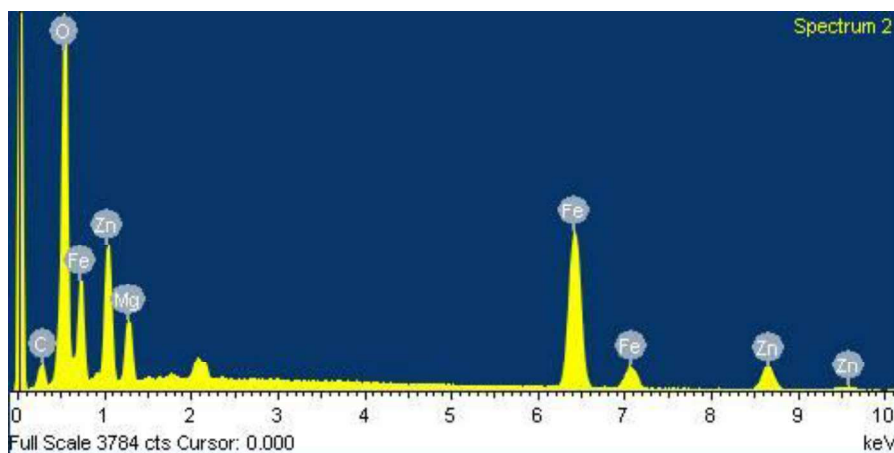


Fig. 4: EDX spectrum for nanosized  $Mg_{0.7}Zn_{0.3}Fe_2O_4$ .

### 3.5. Gas sensing properties

To investigate gas-sensing properties, nanocrystalline  $Mg_{0.7}Zn_{0.3}Fe_2O_4$  powder was made in the form of thick films. The prepared films were then subjected for studying their sensitivity and selectivity at the different controlled temperatures towards various gases in the dynamic setup

Selectivity is another important parameter of gas sensor. The Gas Response (S) against various reducing gases is shown in Fig. 5. The bar graph shows that this material is highly selective towards ammonia as compared with the other reducing test gases. On the bar graph, the time required for sensing of each gas with their 100 ppm concentration is mentioned.

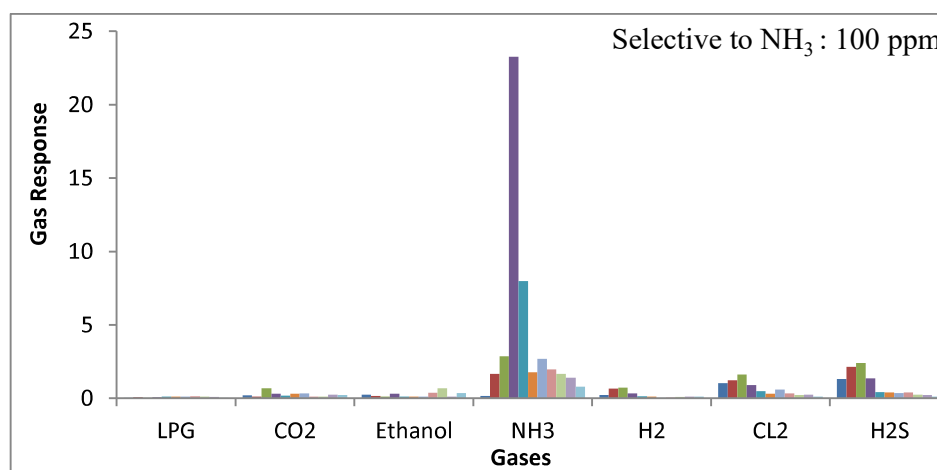


Fig. 5: Response of nanocrystalline  $Mg_{0.7}Zn_{0.3}Fe_2O_4$  towards 100 ppm of various gases at 200°C.

All the gases such as hydrogen, LPG, hydrogen sulphide, CO<sub>2</sub>, Cl<sub>2</sub> and ethanol vapors show response (S) below 5 while ammonia shows 23.26, moreover it requires remarkably less time for sensing as compared with other reducing gases. So, Mg<sub>0.7</sub>Zn<sub>0.3</sub>Fe<sub>2</sub>O<sub>4</sub> can be potential candidate for selective detection of 100 ppm ammonia at 200°C.

Fig. 6 shows response (S) towards ammonia at various operating temperatures which indicates 200°C as the optimum temperature for the gas response. The sensor response to target gas depends on different parameters such as crystallite size, thickness, oxygen adsorption, charge mobility, lattice defects, surface state, porosity, etc.

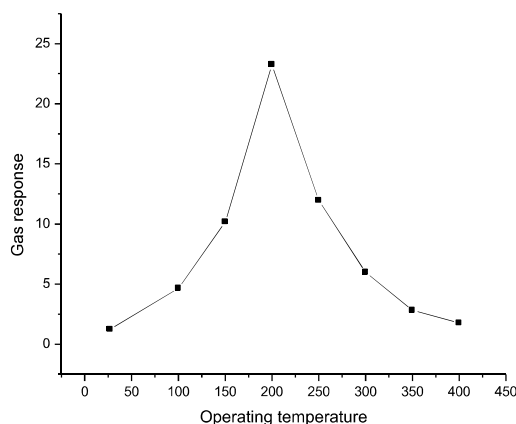


Fig. 6: Response of nanosized Mg<sub>0.7</sub>Zn<sub>0.3</sub>Fe<sub>2</sub>O<sub>4</sub> towards ammonia at the different operating temperatures.

The detailed mechanism of different gases inducing the different resistance change observed is not completely understood at present. The structural features of the nanoscale ferrite complicate the sensing activities, as it involves size, crystallite shape, phase composition, mixed valence and its surface architecture. In the gas sensing mechanism adsorbed O<sup>-</sup> and O<sup>2-</sup> species play important role which in turn depends upon the temperature and oxidation states of the surface ions. The selectivity shown by nanocrystalline Mg<sub>0.7</sub>Zn<sub>0.3</sub>Fe<sub>2</sub>O<sub>4</sub> towards ammonia in comparison with LPG can be attributed to the higher electron affinity of ammonia towards the acidic ferrite surface. At the same time presence magnesium on the surface also increases the acidity therefore may hinder affinity towards LPG and thereby reduce the LPG sensitivity.

In Fig. 7 response towards higher concentrations of ammonia is shown, which indicates that Mg<sub>0.7</sub>Zn<sub>0.3</sub>Fe<sub>2</sub>O<sub>4</sub> responses as low as 20 ppm of ammonia and the response increases linearly with its concentration. The linear relationship between the response and ammonia concentrations suggests that the sensor response exhibits a good dependence on the ammonia concentration.

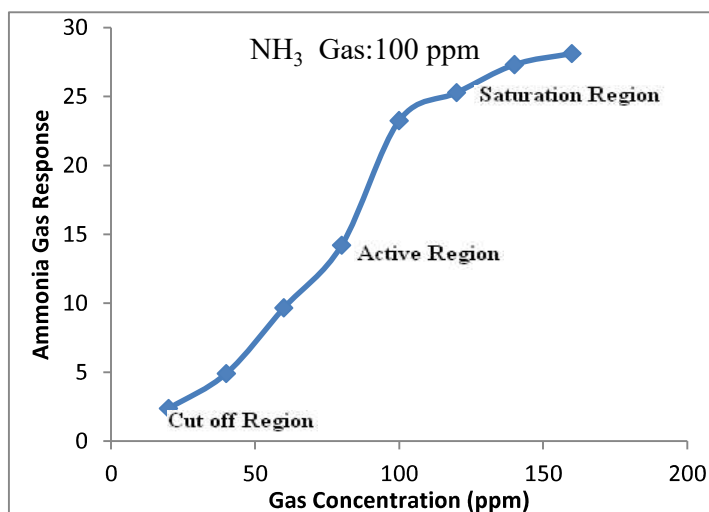


Fig. 7: Response towards various concentrations (ppm) of ammonia.

Fig. 8 shows ammonia response and recovery (as the change in resistance) with reference to time.

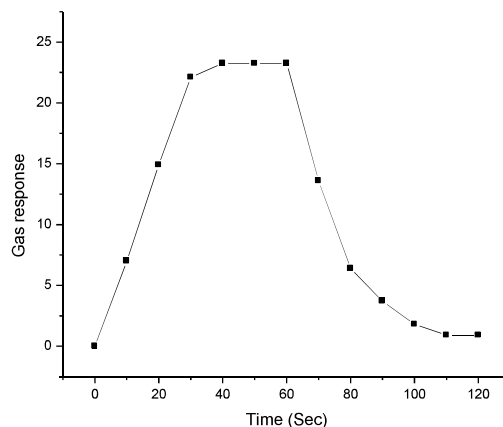


Fig. 8: Response and recovery characteristics of  $Mg_{0.7}Zn_{0.3}Fe_2O_4$  to 100 ppm ammonia.

The nanosized  $Mg_{0.7}Zn_{0.3}Fe_2O_4$  senses 100 ppm of ammonia with response characteristic was good, the resistance of the sensor obviously increased, and the response time was quick and the recovery time was fast. Fast response characteristics may be attributed to the fast interaction of gas molecules with the sensor surface.

In order to study the stability of sensor element, sensor response of  $Mg_{0.7}Zn_{0.3}Fe_2O_4$  to 100 ppm  $NH_3$  was measured by repeating the tests up to the period of 30 days at the time interval of 5 days from initial measurement. The result indicates that  $Mg_{0.7}Zn_{0.3}Fe_2O_4$  based thick film sensor element possesses a very good stability.

#### IV. CONCLUSIONS

Nanopowder of  $Mg_{0.7}Zn_{0.3}Fe_2O_4$  was synthesized using less expensive, environment-friendly and low temperature sol-gel route using citric acid as anionic surfactant occurring at a temperature  $700^\circ C$ . XRD pattern reveals that the synthesized ferrite consists of nanocrystalline particle with average crystallite size 30 nm. SEM analysis validated the structure of final

powder with the grain size  $\sim 125$  nm. The nearly cubical shaped morphology with the isolated nanoparticles shows potential of this simple method. The sensor based on the pure  $\text{Mg}_{0.7}\text{Zn}_{0.3}\text{Fe}_2\text{O}_4$  nanomaterial demonstrated selective response towards 100 ppm of ammonia at  $200^\circ\text{C}$  with a response time of few seconds and good reproducibility. On account of good characteristics mentioned above, nanocrystalline  $\text{Mg}_{0.7}\text{Zn}_{0.3}\text{Fe}_2\text{O}_4$  is a promising material for detection of ammonia.

#### ACKNOWLEDGEMENT

Auhtor(s) would like to thank Sophisticated Analytical Instrument Facility (SAIF), Indian Institute of Technology (I.I.T.), Bombay for carrying out FT-IR, SEM-EDAX and TEM-ED characterizations and Department of Physics, Vidyabharati Mahavidhyalaya, Amravati for providing the XRD facility.

#### REFERENCES

- [1] L. Satyanarayana, K. M. Reddy, V. M. Sunkara, "Nanosized spinel  $\text{NiFe}_2\text{O}_4$ : A novel material for the detection of liquefied petroleum gas in air", *Mater. Chem. Phys.*, vol. 82, pp. 21-26, 2003
- [2] Y. Liu, H. Wang, Y. Yang, Z. Liu, H. Yang, G. Shen, R. Yu, "Hydrogen sulfide sensing properties of  $\text{NiFe}_2\text{O}_4$  nanopowder doped with noble metals", *Sens. Actuators B*, vol. 102, pp. 148-154, 2004.
- [3] T. S. Zhang, P. Xing, J. C. Zhang, L.B. Kong, "Ethanol-sensing characteristics of cadmium ferrite prepared by chemical coprecipitation", *Mater. Chem. Phys.*, vol. 61, pp. 192-198, 1999.
- [4] L. Satyanarayan, K. M. Reddy, S.V. Manorama, "Synthesis of nanocrystalline  $\text{Ni}_{1-x}\text{Co}_x\text{Mn}_x\text{Fe}_{2-x}\text{O}_4$ : a material for liquefied petroleum gas sensing", *Sens. Actuators B*, vol. 89, pp. 62-67, 2003.
- [5] L. Satyanarayan, K. M. Reddy, S.V. Manorama, Nanosized spinel  $\text{NiFe}_2\text{O}_4$ : A novel material for the detection of liquefied petroleum gas in air, *Mater. Chem. Phys.*, Vol. 82 (1), pp. 21-26, 2003.
- [6] C.V. Gopal Reddy, S.V. Manorama, V. J. Rao, "Semiconducting gas sensor for chlorine based on inverse spinel nickel ferrite", *Sens. Actuators B*, vol. 55, pp. 90-95, 1999.
- [7] N. Rezlescu, N. Iftimie, E. Rezlescu, C. Doroftei, P. Popa, "Semiconducting gas sensor for acetone based on the fine grained nickel ferrite", *Sens. Actuators B*, vol. 114, pp. 427-432, 2006.
- [8] C. Xiangfeng, J. Dongli, Z. Chenmou, "The preparation and gas-sensing properties of  $\text{NiFe}_2\text{O}_4$  nanocubes and nanorods", *Sens. Actuators B*, vol. 123, pp. 793-797, 2007.
- [9] Alaud Din, Kalsoom Akhtar, Kh. S. Karimov, Noshin Fatima, Abdullah M. Asiri, M.I. Khan, Sher Bahadar Khan, " $\text{Fe}_2\text{O}_3$ - $\text{Co}_3\text{O}_4$  nanocomposites based humidity and temperature sensors", *J. Mol. Liq.*, vol. 237, pp. 266-271, 2017.
- [10] Safi Asim Bin Asifa, Sher Bahadar Khan, Abdullah M. Asiri, "Assessment of graphene oxide/MgAl oxide nanocomposite as a non-enzymatic sensor for electrochemical quantification of hydrogen peroxide", *J. Taiwan Inst. Chem. Eng.*, vol. 74, pp. 255-262, 2017.
- [11] Alaud Din, Kh. S. Karimov, Kalsoom Akhtar, M.I. Khan, Muhammad Tariq Saeed Chani, Murad Ali Khan, Abdullah M. Asiri, Sher Bahadar Khan, "Impedimetric humidity sensor based on the use of  $\text{SnO}_2$ - $\text{Co}_3\text{O}_4$  spheres", *J. Mater. Sci. Mater. Electron.*, vol. 28, pp. 4260-4266, 2017.
- [12] Alaud Din, Sher Bahadar Khan, M.I. Khan, Safi Asim Bin Asif, Murad Ali Khan, Saima Gul, Kalsoom Akhtar, Abdullah M. Asiri, "Cadmium oxide based efficient electrocatalyst for hydrogen peroxide sensing and water oxidation", *J. Mater. Sci. Mater. Electron.*, vol. 28 (1) pp. 1092-1100, 2017.
- [13] Muhammad Tariq Saeed Chani, Khasan S. Karimov, Sher Bahadar Khan, Abdullah M. Asiri, "Fabrication and investigation of cellulose acetate-copper oxide nano-composite based humidity sensors", *Sensor Actuator Phys.*, vol. 246, pp. 58-65, 2016.
- [14] Sher Bahadar Khan, Khasan S. Karimov, Muhammad Tariq Saeed Chani, Abdullah M. Asiri, Kalsoom Akhtar, Noshin Fatima, "Impedimetric sensing of humidity and temperature using  $\text{CeO}_2$ - $\text{Co}_3\text{O}_4$  nanoparticles in polymer hosts", *Microchimica Acta*, vol. 182 (11-12), pp. 2019-2026, 2015.
- [15] P.J.D. Peterson, A. Aujla, K.H. Grant, A.G. Brundle, M.R. Thompson, J.V. Hey, R.J. Leigh, "Practical Use of Metal Oxide Semiconductor Gas Sensors for Measuring Nitrogen Dioxide and Ozone in Urban Environments", *Sensors*, vol. 17, pp. 1653-1677, 2017.
- [16] G. Korotcenkov, "Gas response control through structural and chemical modification of metal oxide films: state of the art and approaches", *Sensor. Actuator. B*, vol. 107, pp. 209-232, 2005.
- [17] C.C. Wang, A.A. Akbar, M.J. Madou, "Ceramic based resistive sensors", *J. Electroceram.*, vol. 2 (4), pp. 273-282, 1998.



- [18] B. B. Dora, S. Kumar, R. K. Kotnala, B. C. Raulo, M. C. Sahu, "Improved Magnetic Properties of Ni-Zn Nano Ferrites by Using Aloe vera Extract Solution", Int. J. Pharm Sci. Rev. Res., vol. 30 pp. 294-298, 2015.
- [19] A. M. El-Sayed, "Influence of zinc content on some properties of Ni-Zn ferrites", Ceramic Inter., vol. 28, pp. 363-367, 2002.
- [20] S. V. Kakatkar, S. S. Kakatkar, R. S. Patil, A. M. Sankpal, S. S. Suryavanshi, D. N. Bhosale, S. R. Sawant, "X-Ray and Bulk Magnetic Properties of the Ni-Zn Ferrite System", Phy. Stat. Sol.(b), vol. 198, pp. 853, 1996.